OPTIMIZATION AND COMPARISON OF BACK IRON BASED COUPLING ARCHITECTURES FOR ELECTROMAGNETIC VIBRATION TRANSDUCERS USING EVOLUTION STRATEGY

D. Spreemann[1], Alexander Willmann[1], Bernd Folkmer[1] and Yiannos Manoli[1,2]
[1]HSG-IMIT Institute of Micromachining and Information Technology
[2]Chair of Microelectronics, Department of Microsystem Engineering (IMTEK) University of Freiburg

Abstract: This paper presents the optimization of two different back iron based coupling architectures for electromagnetic vibration transducers using evolution strategy. The objective function is thereby both the maximum output power and the maximum output voltage. As a final conclusion the performance limits of the architectures are compared to five different previous presented architectures without back iron. It is shown that the presented loudspeaker based architectures are capable of generating the highest output power and output voltage levels. Experimental results obtained with a measurement set-up have been used to verify the simulation models. With the presented results the designer of electromagnetic vibration transducers gets a guideline which architectures are capable of generating the highest output power and output voltage in a construction volume of 1 cm³.

Keywords: vibration transducer, evolution strategy optimization, coupling architecture, comparison

INTRODUCTION

In the recent years a lot of work has been done in the field of electromagnetic vibration energy harvesting devices. Thereby a lot of different electromagnetic coupling architectures have been applied by numerous research facilities [1]. However in the multiplicity of publications the selection criterion of the appropriate coupling architecture is often omitted. Beyond this the geometrical parameters of the magnet, the coil and if existent the back iron parts are in the most of all cases based on rough simplifying analytical assumptions, experience if not intuition. In [2] five different commonly used architectures without back iron has been optimized and compared in a construction volume of 1 cm³ and it has been shown that the output performance is strongly dependent on the architecture. Moreover the appropriate dimensioning of the components has a significant influence as well. In the same manner this paper extends the list of architectures with two back iron based architectures (in the following abbr. A VI and A VII) that are typically used in moving coil loudspeakers [3] (Fig. 1). In a first step the geometrical parameters of these architectures will be optimized in a construction volume of 1 cm³ using evolution strategy (ES) optimization technique. The objective function is thereby both the maximum output power and the maximum output voltage. The applied boundary conditions, based on mesoscale vibration transducers are the same as in [2]. Due to this the output performance of all the architectures will afterwards directly be compared. Experimental

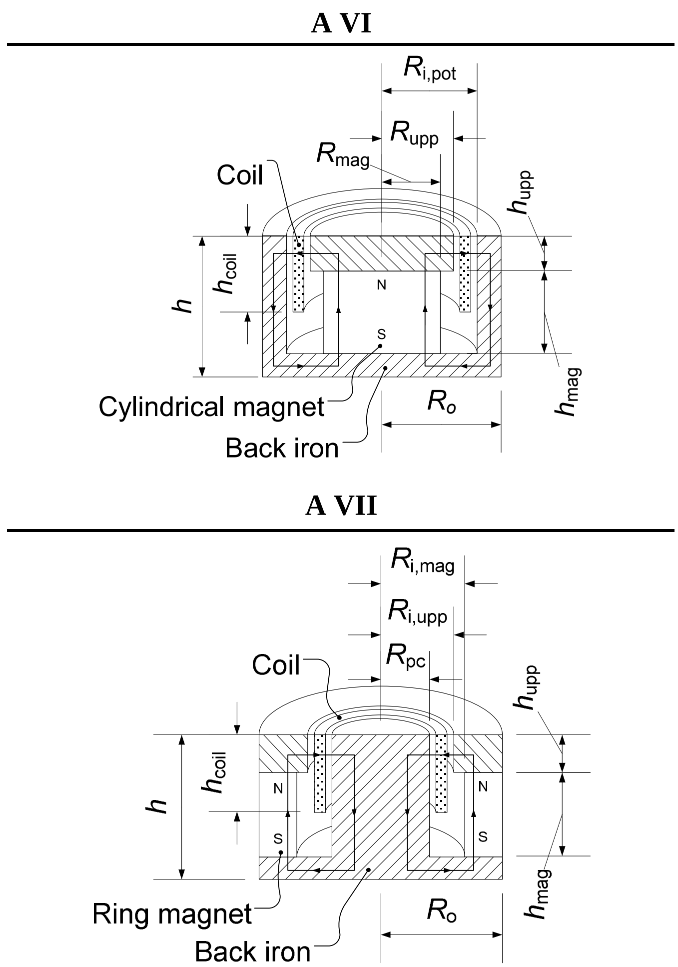

Fig. 1: Half-section of the considered coupling architectures. Architecture A VI is based on a cylindrical magnet in spite to the ring magnet in A VII. The closed loop indicates the magnetic circuit.

data obtained with a measurement set up are used to verify the simulation models. The paper concludes with a comparison of all the architectures considered in this paper and in [2] (architectures with and without back iron). This comparison reveals the architectures which are inherently capable of generating the highest output power and output voltage levels.

EVOLUTION STRATEGY OPTIMIZATION

As stated in the introduction the aim of the presented optimization is to find geometrical parameter sets that yield maximum output power and output voltage respectively in a construction volume of 1 cm³ (defined by R_o=6mm and h=8.9mm). The construction volume contains the magnet, the coil and the back iron parts at its resting position. This is because the spring, the housing, circuit boards and other components of the transducer may be implemented in several ways. Note that in the optimization simulations the coil is flush with the upper pole plate. However in application this might be different in order to attach the coil at the housing.

From Fig. 1 it is evident that the geometrical parameters yield a 6-dimensional search space which can conveniently be explored using ES optimization technique. In this request the $(\mu+\lambda)$ selection mechanism is applied [4]. The fitness (output power respectively output voltage) is calculated using the calculation procedure in [2]. The only difference is that instead of the analytical calculation of the magnetic field 2D/axysymetric static magnetic finite element analyses have been applied to compute the mean value of the magnetic flux density B_{mean} in the air gap at the resting position of the oscillating mass (magnet and back iron parts). Therewith the induced open circuit electromotive force ε (emf) is given by:

$$\varepsilon = -NB_{mean} l\dot{z} = -k_t \dot{z}\,, \qquad (1)$$

where N is the number of coil windings, l the mean circumference of the coil, $\dot{z}$ the velocity of the oscillating mass and k_{t} the transduction factor. A typical convergence of an optimization run is shown in Fig. 2. Therein the mean value of the fitness (in this example the output power) of the selected individuals is plotted versus the number of generations. In the first generation the fitness of the selected individuals is rather poor and the individuals are randomly spread in the search space. In the intermediate state (generation 5-15) the individuals are still rather different but first properties have already been asserted (i.e. $R_{\text{mag}}=R_{\text{upp}}$ in A VI and $R_{\text{i,mag}}=R_{\text{i,upp}}$ in A VII). Consequently after circa 60 generations there

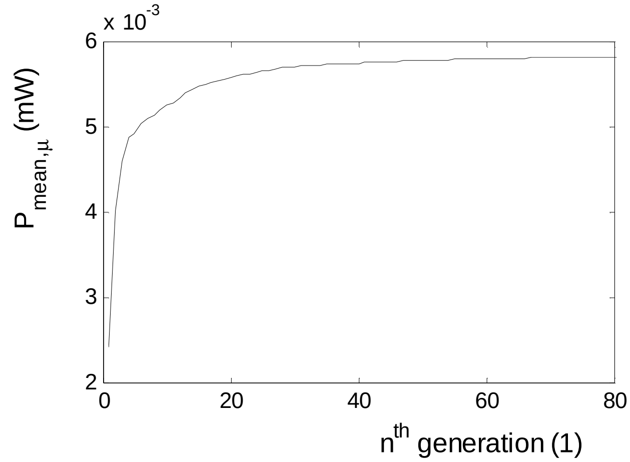

Fig. 2: Typical convergence of an evolution strategy optimization run. The plot shows the mean value of the output power of the selected individuals versus the generation.

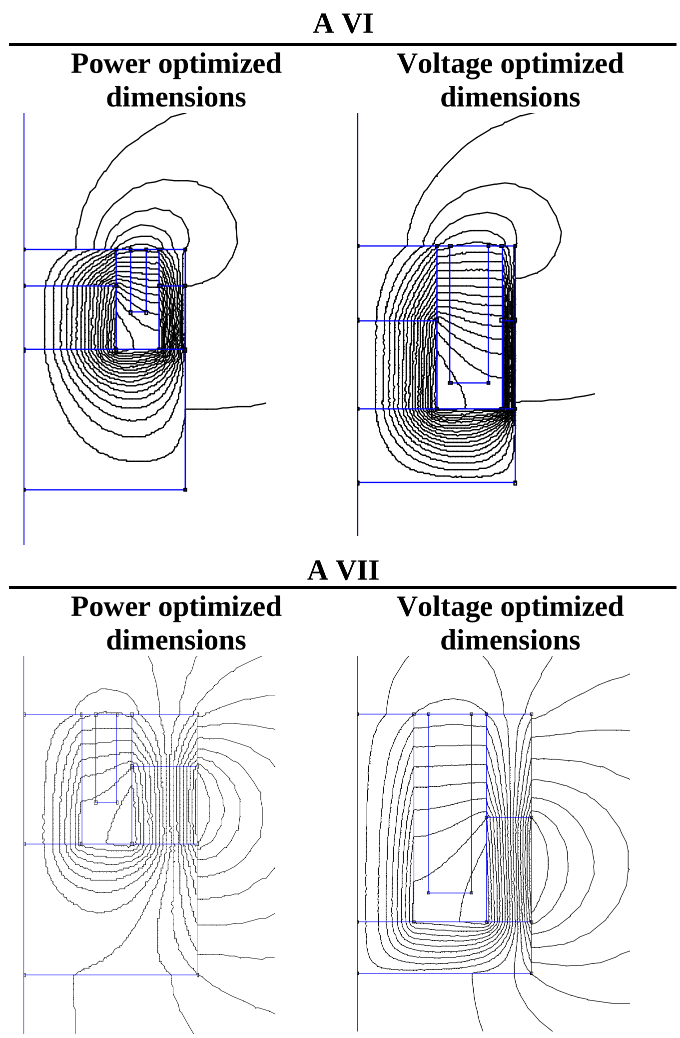

Fig. 3: Right half of the flux distribution for optimal dimensions of the geometrical parameters with respect to the output power and the output voltage.

is no significant increase of the output power for further generations and the optimization converges. At this point the individuals are rather similar and can be expected to represent an optimal solution in the search space. Fig. 3 shows the architectures with optimized dimensions for both maximum output power and maximum output voltage. With A VI a maximum output power of 5.81 mW can be generated at a voltage level of 1.73 V and a maximum output voltage of 3.14 V at a power level of 3.25 mW. The coil volume of the output power optimized design (37 mm³) is more than 5 times smaller than the volume of the output voltage optimized design (195 mm³). With A VII a maximum output power of 6.72 mW can be generated at a voltage level of 1.99 V and a maximum output voltage of 3.49 V at a power level of 4.00 mW. Just as for A VI the coil volume of the output power optimized design (38 mm³) is again almost 5 times smaller than the volume of the output voltage optimized design (179 mm³). Note that it is in general advantageous if the radius of the magnet equals the radius of the upper pole plate ($R_{mag}=R_{upp}$ in A VI and $R_{i,mag}=R_{i,upp}$ in A VII).

EXPERIMENTAL ANALYSIS

The verification of the simulation models was conducted using a measurement set-up which is based on a vibration shaker unit with accelerometer feedback. A schematic of the measurement set-up is shown in Fig. 4. The magnet and back-iron parts of the architectures have been attached to the shaker whereas the coil has been mounted on a fixed XYZ adjustment unit. Great care was taken to position the coil concentrically in the air gap. Afterwards the shaker was forced to vibrate at predefined controlled amplitude of 50 µm at 100 Hz. At different depths of immersion *x* the emf amplitude is measured using an oscilloscope. Together with the given velocity of the oscillation the transduction factor is simply given by the rearrangement of (1).

Two different macroscale devices were built and tested for each architecture. These devices differ pairwise only in the dimension of the upper pole plate (h_{upp}). As an example the results of the transduction factor measurement for A VII should be discussed here. A comparison of the measurement to the simulated values is shown in Fig. 5. From there it is apparent that the simulated values are in very good agreement to the measurement results. The used parameters of the A VII device are summarized in table 1. The NdFeB magnet has a residual magnetic flux density of 1.3 T. The coil is made of 40 µm enamelled copper wire with a total resistance of

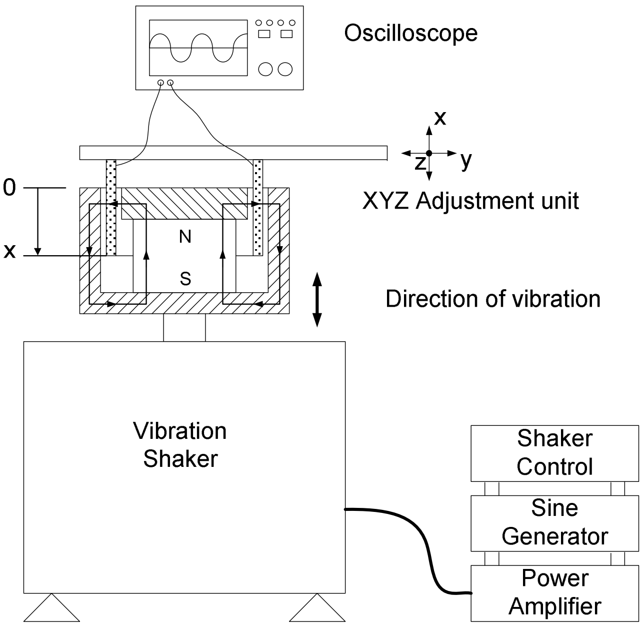

Fig. 4: Schematic of the experimental set-up used to measure the transduction factor at different depths of immersion of the coil.

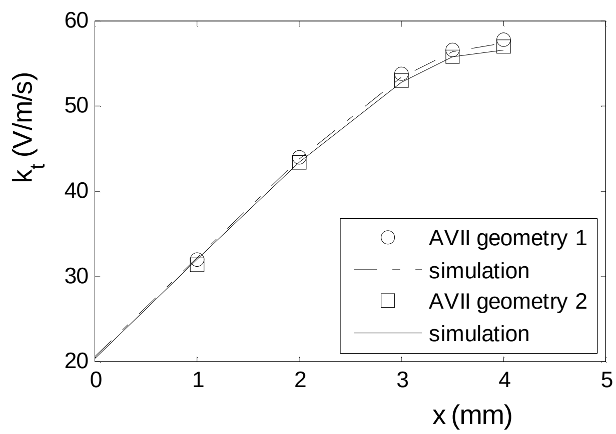

Fig. 5: Measured and predicted transduction factor of A VII for different depths of immersion of the coil.

1260 Ω. The corresponding number of windings can easily be calculated using the resistance per unit length of 13.6 Ω/m. For the back-iron parts standard 1.7011 machining steel (9S20K) is used. Note that the verification measurements with the two A VI macroscale devices results in similar accuracy. However due to lack of space the results are omitted here.

COMPARISON AND CONCLUSION

So far the evolution strategy optimization technique has been applied to the presented loudspeaker based coupling architectures. The optimal

Table 1: Dimensions of the two A VI testing device with different dimensions of the upper pole plate.

Parameter	Value (mm)
R_0	13.5
$R_{i,\mathrm{mag}}$	8
$R_{i,\mathrm{coil}}$	5.80
$R_{o,\mathrm{coil}}$	7.15
$R_{i,\mathrm{upp}}$	7.65
R_{pc}	5.30
h	11
h_{mag}	5
h_{coil}	4.50
h_{upp} geometry 1 / 2	3 / 6

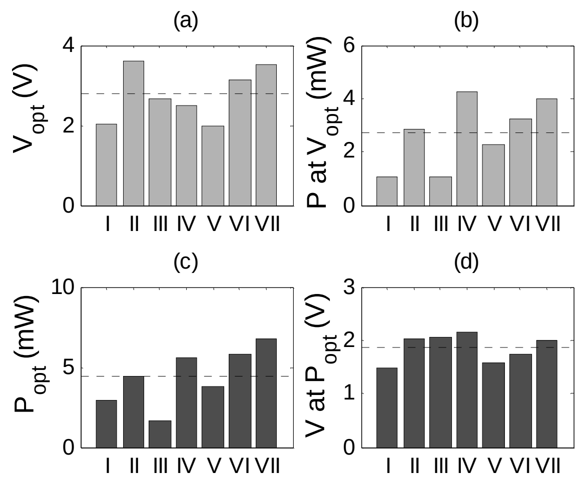

Fig. 6: Comparison of the maximum output performance of the different architectures. (a) maximum output power, (b) voltage level at maximum output power, (c) maximum output voltage and (d) power level at maximum output voltage. The dashed curves indicate the mean value of all architectures.

geometrical dimensions could be defined for both maximum output power and maximum output voltage. Beyond this experimental data obtained with a measurement set-up has been used to verify the simulation models. Fig. 6 comprises the maximum output performance of all the architectures presented in this paper (A VI and A VII) as well as the maximum output performance of the previous presented architectures (A I-V). First of all the comparison shows that A VII performs slightly better than A VI either for output power and output voltage generation. The ring magnet based architecture should therefore be favoured whenever possible. Moreover the highest possible output voltage of all the considered architectures is obtained with A II. In A II a cylindrical magnet oscillates towards a cylindrical coil without immersion. However even though the maximum output voltage of the presented architectures are slightly lower the output power levels at the maximum output voltages are obviously higher. For A VII this advantage (40% higher output power at almost the same output voltage) definitely compensates this drawback. Concerning the output power generation the presented architectures perform best. Taking the voltage level at the maximum output power into account A VII remains at the first place. However in the strict sense A IV is capable of generating the same power level as A VI even though the voltage level at the maximum output power point is noticeably higher (25%). In summary A IV, which consists of four opposite polarized rectangular magnets which oscillates across a coil, has therefore the better output performance than A IV. Altogether the back iron based coupling architecture A VII has the best output performance of all the considered architectures. Nevertheless this comparison study is based on the maximum output performance which is certainly the most important characteristic. However, depending on the application, there may be other important characteristics, which need to be taken into account such as the form factor, the magnetic field distribution outside the generator (unwanted nonlinear magnetic forces due to a steel environment), packaging, potential in MEMS implementation and so on. Furthermore the order of the architectures is only valid for optimized dimensions. That means that an unfavourable dimensioned architecture may descend with respect to a proper dimensioned architecture. The dimensioning takes therefore a vital key role in the development of efficient electromagnetic vibration energy harvesting transducers.

ACKNOWLEDGEMENTS

This research was funded by the initiative Zukunftsoffensive III, Land Baden-Württemberg, Germany

REFERENCES

[1] D.P. Arnold, Review of Microscale Magnetic Power Generation, *IEEE Transactions on magnetics*, **vol. 43**, no. 11, S3940–3951, 2007

[2] Spreemann D, Folkmer B, Manoli Y, 2008 Comparative study of electromagnetic coupling architectures for vibration energy harvesting devices *Technical Digest PowerMEMS 2008 (Sendai, Japan, 9–12 November 2008)* 257–260

[3] Eargle J 2003 *Loudspeaker Handbook* 2^{nd} *ed.* (Massachusetts, Kluwer Academic Publishers)

[4] T. Bäck 1996 *Evolutionary Algorithms in Theory and Practice* (Oxford, Oxford University Press).